Supporting Information

Chan et al. 10.1073/pnas.0906549106

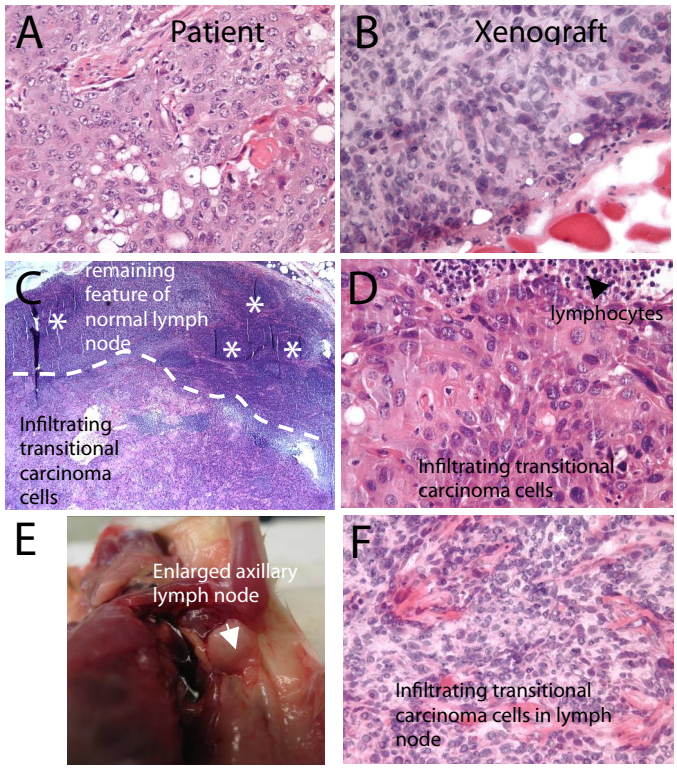

Fig. S1. Histological analysis of representative bladder cancer (BC-8; pT3a pN1 pMX) and serially derived xenograft tumor and lymph node metastasis. (*A*) H&E staining of primary bladder cancer sample (BC-8). (*B*) H&E staining of xenograft tumor formed from BC-8. (*C* and *D*) H&E staining of lymph node from BC-8 that was infiltrated with transitional carcinoma cells (*asterisks in C*).(*E*) Photograph showing an enlarged axillary lymph node (*arrow*) in *RAG2*$^{-}$/γc^{-} mice that was engrafted with transitional carcinoma cells from BC-8. (*F*) H&E staining of axillary lymph node from mouse showing typical histology of transitional cells.

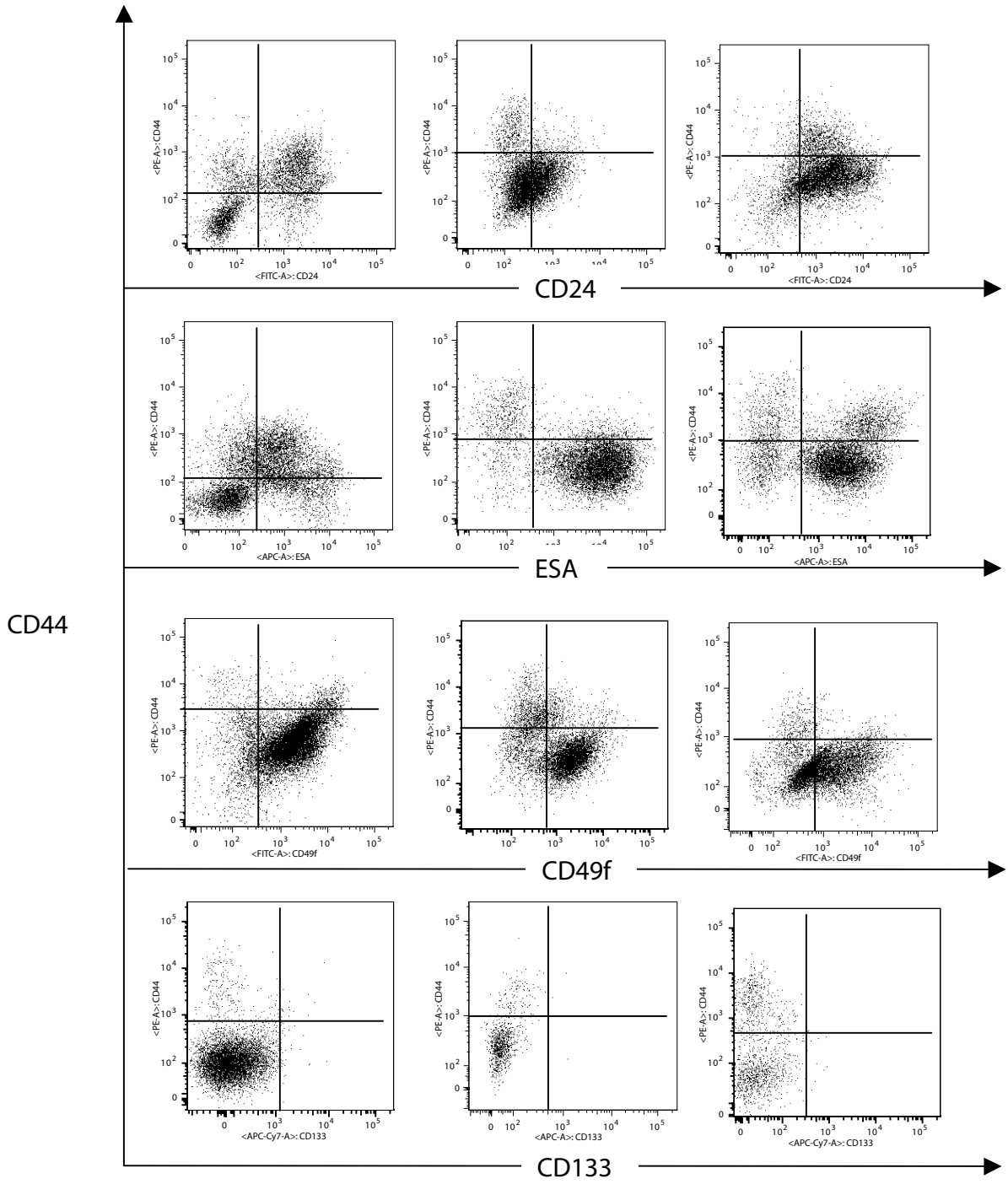

Fig. S2. Flow cytometry analysis of stem cell-related cell-surface markers. Bladder tumors were enzymatically dissociated into cell suspensions and analyzed by FACS (Becton Dickenson). Infiltrating hematopoietic cells ($CD45^+$) and endothelial cells ($CD31^+$) were excluded, and the relative expression of CD44, CD24, ESA, CD49f, and CD133 from representative bladder tumors is shown.

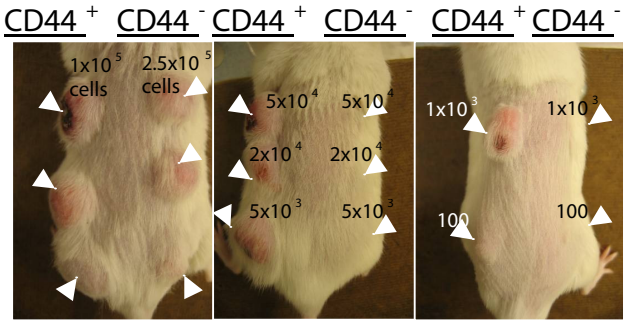

Fig. S3. Representative photographs demonstrating the engraftment of tumors (*arrowheads*). Bladder tumor cell subpopulations ($CD44^{+}/CD44^{-}$) in limiting dilutions were injected intradermally into $RAG2^{-}/\gamma c^{-}$ mice.

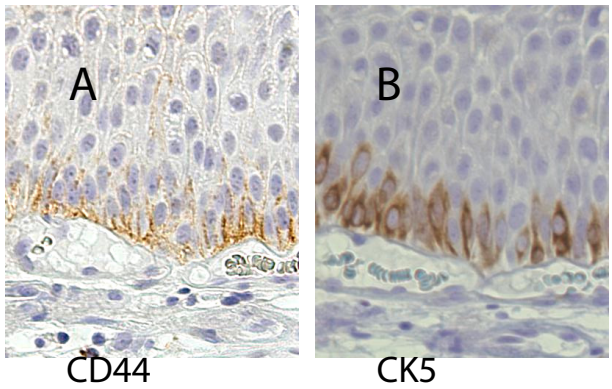

Fig. S4. Immunohistochemical analysis of (*A*) CD44 and (*B*) CK5 in normal human urothelium. Brown color indicates positive staining.

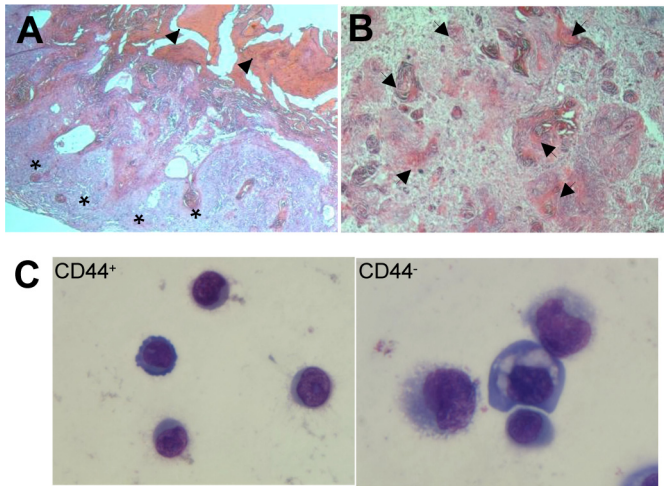

Fig. S5. (*A*) Hematoxylin and Eosin (H&E) staining of a representative xenograft tumor formed from patient $CD44^+$ tumor cells. Tumor comprises areas with less differentiated (indicated by *) and terminally differentiated tumor cells (indicated by arrows). (*B*) H&E staining of a representative xenograft tumor formed from patient $CD44^-$ tumor cells, comprising of highly keratinized, terminally differentiated cells (indicated by arrows). (*C*) Giemsa-Wright staining showing the cellular morphology of fractionated $CD44^+$ and $CD4^-$ tumor cells from representative bladder cancer (BC-3).

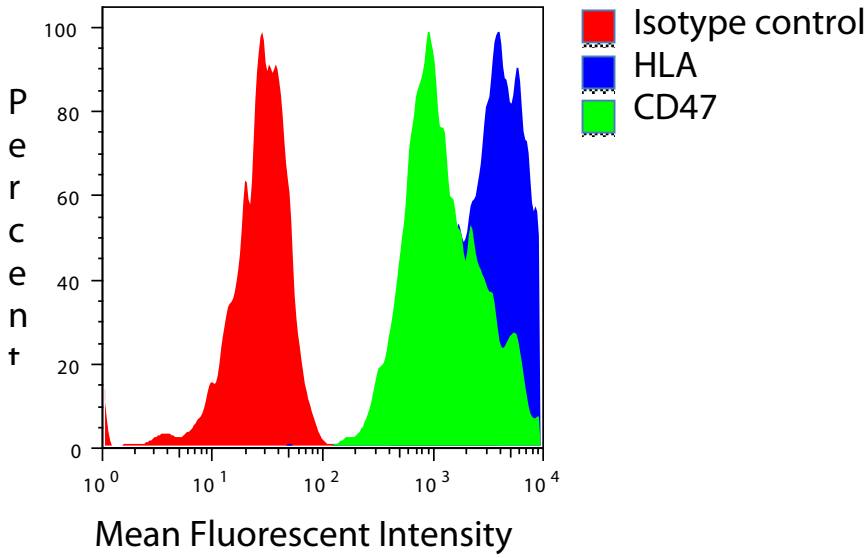

Fig. S6. Flow cytometry analysis of a representative human bladder cancer (BC-8) demonstrating the binding of CD47 and HLA antibodies to bladder cancer cells over isotype control.

Table S1. Bladder cancer patient information in relation to their relative engraftment ability in *RAG2*$^{-}$/γc^{-} mice

Patient identifier	TNM staging	% CD44^{+} cells	Tumor engraftment in vivo	Serially transplantable tumor in vivo
BC-12	pT3b pN2 pMX	34.5	Yes	No
BC-1	pT3b pN0 pMX	7.8	Yes	Yes
BC-2	pT3a pN2 pMX	3.06	No	No
BC-8	pT3a pN1 pMX	6.03	Yes	Yes
BC-11	pT3a pN0 pMX	27.9	Yes	No
BC-9	pT3a pN0 pMX	24.5	No	No
BC-5	pT2b pN0 pMX	36.3	No	No
BC-7	pT2b pN0 pMX	6.5	No	No
BC-6	pT2a pN0 pMX	8.9	Yes	No
BC-4	pT2a pN0 pMX	0	No	No
BC-10	pT2a pNX pMX	3.4	No	No
BC-14	pTa pN0 pMX	7.8	No	No
BC-13	pTis pN0 pMX	5.48	No	No
BC-3	N/A	4.8	No	No

Bladder cancer TNM stages ranked from highest to lowest according to the ability of tumor cells to form xenograft tumors in *RAG2*$^{-}$/γ c^{-}mice. Of 14 freshly isolated bladder cancers collected, 12 were muscle invasive (pT2 and pT3 stage), 1 was a carcinoma in situ (pTis), and for 1 tumor clinical information was lacking. Four of 6 pT3-stage tumors engrafted, 1 of 5 pT2-stage tumors engrafted, and no tumor below pTa stage engrafted. Two tumors were serially transplantable in vivo, both of which were at pT3 stages.

Table S2. Percentage of tumor cells co-expressing CD44 and K5 or K20

Marker expression	% cells
$CD44^{+}K5^{+}$	37
$CD44^{+}K5^{-}$	7
$CD44^{-}$ $K5^{+}$	10
$CD44^{-}$ $K5^{-}$	46
$CD44^{+}K20^{+}$	3
$CD44^{+}K20^{-}$	39
$CD44^{-}$ $K20^{+}$	28
$CD44^{-}$ $K20^{-}$	30

Percentage of bladder tumor cells co-expressing CD44 and/or cytokeratin 5/20. Bladder xenograft tumors ($n = 4$) were analyzed for the percentage of cells expressing or co-expressing the markers CD44, CK5, and CK20 by immunofluorescence staining.